Biophysical Journal, Volume *116*

Supplemental Information

High-Copy-Number Plasmid Segregation—Single-Molecule Dynamics in Single Cells

Tai-Ming Hsu and Yi-Ren Chang

Supporting Material

High-copy-number plasmid segregation – single-molecule dynamics in single cells

*T.-M. Hsu and Y.-R. Chang**

Plasmid construction

All plasmids were constructed using the In-Fusion Cloning method (Clontech Laboratories, Inc., USA). With this method, plasmids can be directly and directionally constructed in one step from multiple linear DNA fragments with designed overlap. The linear DNA fragments were amplified by PrimeSTAR MAX DNA polymerase (Takara Bio Inc., Japan) to provide fidelity up to 10 kb.

To construct plasmid pTetORK34b, several steps were required. First, an intermediate plasmid pTetR4-4m, encoding self-regulated circuitry, P_{tet}*::tetR-myfp*, was designed based on the replication origin from pSOT37, a *cer*-deleted ColE1 derived plasmid, and constructed by direct fusion of the PCR fragments of *tet* promoter from pZS2-123 (1), *tetR* from the chromosome of *E. coli* strain BL21, and the monomeric *myfp* gene. The antibiotic resistance gene *bla* replaced the kanamycin resistance marker from pZS2-123. The tandem repeat sequence of *tetO* from pLAU44 (2), which was digested by restriction enzymes, SphI and SacII, was later fused downstream of *myfp*. The DNA fragment, *L16*, encoding a peptide sequence of TSGSAASAAGAGEAAA, was applied as a linker between *tetR* and *myfp*, and terminator *TSAL2* was inserted between *myfp* and the tandem repeat sequence of *tetO*. Similarly, to construct plasmid pTetORK34p, another intermediate plasmid pTetR4-4p was designed as a derivative of pTetR4-4m with the replacement of P_{RNAII} for P_{phlF}. The plasmid was constructed by self-fusion of the PCR-synthesized DNA fragment including the whole plasmid sequence except P_{RNAII}, with additional P_{phlF} sequence instead by the primer extension. Unlike the design reported by Panayotatos (3), the promoter and sequence of *RNAI* were entirely used to preserve its original function of regulating the replication of ColE1.

Plasmid pLacOIC2c was constructed by sequential fusions of the ColE1 replication origin from pSOT37, including the PCR fragments of the *lac* promoter and *lacI* gene from the chromosome of *E. coli* strain MG1655, *mcherry* gene from pZS2-123, and the chlorophenol resistance marker from commercial plasmid pPROtet.E (Clontech Laboratories, Inc., USA). The frame-shift mutation from *lacI* gene to $lacI^{adi}$ was replaced the last 31 codons of the *lacI* gene with 16 codons, preventing $LacI^{adi}$ from forming tetramers (4). The tandem repeat sequence of *lacO* was derived from the digestion of pLAU43 (2) with restriction enzymes, BspHI and SacII.

The single-copy plasmids, pZC320-tetO and pZC320-lacO, were constructed by replacing the lactose-

controlled expression system with DNA fragments [P_{tet}*::tetR-myfp tetO2*x54] (from pTetORK34b) and [P_{lac}*::lacI*^{adi}*-mcherry lacO*x90] (from pLacOIC2c) in the mini-F plasmid pZC320 (5), respectively.

Plasmid p15AA-phlFH.tq was constructed from pJMJ178, a p15A derived plasmid with the arabinose controlled expression system. The chloramphenicol resistance marker was first replaced with the *bla* gene from pMLB1113, and fused *phlF* gene from pAND at the 3'-end of P_{BAD} with a T7 terminator sequence from pZS2-123. The fragments, including a weak constitutive promoter (mutant of Biobrick J23114), an RBS (BioBrick B0034), *hupA* gene from MG1655 and *mturquoise2* gene from pPalmitoyl-mTurquoise2 (Addgene, USA) were inserted between the p15A origin and 3'-end of *araC* in the opposite direction.

Calibration of single-plasmid fluorescence

The numbers of plasmids in cells were estimated based on the intensity of single-copy mini-F plasmids, pZC320-tetO and pZC320-lacO. The intensity of a single plasmid was calculated based on the total fluorescence intensities of single cells divided by the numbers of plasmid copies within, which were identified as individual fluorescent spots. Most instances of possible overlap of fluorescent spots were removed from the calculation. However, due to the comparatively lower resolution of the red fluorescence (longer wavelength), there were still some spots which may have represented more than one plasmid, as suggested by a second peak in the fluorescence intensity distribution. From the center intensity of the peaks, the population of the second peak seems to indicate that the spots included two plasmids, and thus, the second peak spots were removed from the calibration. Note that before all calculations, the background from the cytoplasmic auto-fluorescence and the surrounding environment of the gel pad, measured in BW25113FH cells, was subtracted from the overall intensity of cells.

To minimize differences between measurements, several quality control procedures were applied. For all measurements, the cells in all experiments were cultured in the same batches of LB and M9 medium. The culture conditions (i.e., temperature, time, and cell concentration) were precisely controlled. To keep consistency between gel patches, every gel patch was dissolved in the same batch of M9 medium and freshly prepared before the observation period to prevent water evaporation. Also, a temperature- and humidity-control system was utilized during the microscopic observation to maintain the condition of the gel pads. The cover-slides were washed in neutral detergent for 20 min and rinsed three times in pure water for 10 min with sonication. The cleaned cover-slides were stored and sealed in pure water and then dried in pure nitrogen before use. The alignment of the optical path and the laser powers in the setup of the microscope were finely tuned and kept consistent throughout measurement days. To stabilize the laser power and the temperature of the environment, the whole microscopic system was switched on at least one hour before observations were made. Furthermore, for the fluorescent intensity measurements, the fluorescence background from the gel pad was obtained in a region near each cell (5-μm distance around the cell boundary), and the fluorescence deviation between the gel pads was found to be approximately 5%. The cellular auto-fluorescence was

obtained from the average intensity of BW25113FH cells after removing the gel-pad background. The BW25113FH cells were cultured in parallel and spread on the same batch of gel pads on each day of measurement. After subtracting the intensities of the fluorescence background and the auto-fluorescence, the intensity contribution of the plasmids in each cell was obtained as the summation of the intensity of the pixels within the cells. The efficiency of the background subtraction was confirmed based on measurements of BW25113FH cells transformed with single-copy plasmids, pZC320-tetO and pZC320-lacO. The intensity background of these cells can be directly obtained from all the pixels in the cell aside from those identified as plasmids by 2D Gaussian fitting (~6 pixels in length).

The reproducibility of the experimental setup was examined by imaging fluorescent microspheres. In this examination, 0.1-μm fluorescent microspheres (ThermoFisher Scientific, TetraSpeck™ Microspheres) were diluted with M9 medium and spread on the gel pads. The deviation between the average fluorescence intensities of the microspheres in different gel pads was 4%, which agrees with the measured deviation between the gel pads. Thus, 4% also represents an estimation of the systematic deviation between single measurements introduced by the experimental procedure.

The numbers and the standard errors of the plasmids in a single cell were predicted as follows. Assume a number of plasmids N in a cell. The fluorescence intensity of this cell after removing the background can be statistically predicted as $F = N F_1 \pm N^{1/2}\Delta F_1$, where F_1 and ΔF_1 are the mean and the standard deviation of the measured intensity of cells containing single plasmids (**Figure S1B**). Therefore, in our experiments, from the measured fluorescent intensity F in a cell, the number of plasmids N and the uncertainty ΔN of plasmids can be approximated by $N \pm \Delta N \sim (F / F_1) \pm (\Delta F_1 / F_1) (F / F_1)^{1/2}$. From **Figure S1B**, the relative deviations between single plasmids $\Delta F_1/F_1$ were 30% and 37% for [P_{tet}*::tetR-myfp tetO2*x54] and [P_{lac}*::lacI*^{adi}*-mcherry lacO*x90] cassettes, respectively. Compared to the systematic deviation, the deviations between single plasmids should be majorly derived from the board occupancy rate of the *tetO* and *lacO* arrays. Note that since the number of the plasmids should be naturally an integer, the number of plasmids N is presented as the nearest integer of the value of (F / F_1). Regarding the uncertainty, in a single measurement from a single cell, if the predicted number of plasmids is 40, for instance, the uncertainty will be roughly 7. In another example related to the cells in the replication repression experiments (**Figure 1C** and **1D**), the numbers of plasmid pTetORK34p were often only a few; the uncertainty would be 2 in a cell with a predicted plasmid number of 4. With regard to the experiments on single plasmid tracking, in order to ensure the tracked fluorescent spots actually represent single plasmids, only the spots with intensities less than F_1 and fitted spot widths less than 250 nm were considered. According to the results of the single *tetO* tandem array (**Figure S1B**, $F_1 \pm \Delta F_1 \sim 74000 \pm 22000$), a fluorescent spot representing two plasmids will have a predicted fluorescence of $F \pm \Delta F \sim 148000 \pm 31000$, and the respective probability that the apparent fluorescence is less than F_1 would be statistically less than 2.5%.

The average total numbers of pTetORK34b and pLacOIC2c in a host cell (*E. coli* BW25113FH) were 42 ± 2 (mean ± SE, $N_{cell} = 150$), which was verified by quantitative PCR (~40 plasmids per cell, **Figure S3**), following a similar procedure as used in a previous report (6). This number also agrees with the earlier measurements made by quantitative PCR and super-resolution imaging (6, 7). Likewise, the numbers of pZC320-tetO and pZC320-lacO measured by quantitative PCR were approximately 1 (**Figure S3**), validating the appropriateness for these two plasmids to be used as unit calibrations of the fluorescent intensities of single cassettes. The standard errors of the average numbers of plasmids within a single cell were obtained from the uncertainty of each measurement and the statistics of the samples. The experimental uncertainty of the inherited plasmid numbers in daughter cells is similarly calculated by accounting into the uncertainties in all single measurements.

Influence of FROS system

The interaction between plasmids due to FROS cassettes, i.e., additional affinity or repulsion, was examined based on the inheritance of the co-transformed pTetORK34b and pLacOIC2c in the host cells (**Figure 1B** and **S1A**). Two selection markers, kanamycin and chloramphenicol, were respectively encoded in pTetORK34b and pLacOIC2c for the co-transformation experiments (8). As shown in **Figure S1C**, the correlation coefficient between quantity ratios ($N_{P1,D}/N_{P1,P}$ and $N_{P2,D}/N_{P2,P}$) is approximately 0.22, where $N_{P1,P}$, $N_{P2,P}$, $N_{P1,D}$ and $N_{P2,D}$ are the parental and inherited quantities of the plasmids pTetORK34b and pLacOIC2c, respectively. The weak correlation between these two inherited populations suggests the FROS cassettes are independent with regard to plasmid segregation, and the plasmids encoded in these two cassettes can be considered to be physiologically identical in the host cells.

Incompatibility of ColE1 origin

The ability to observe the trajectories of single plasmids requires that the cells contain only a few copies of optically resolvable pTetORK34b or pLacOIC2c. Statistical analysis of the quantities of these two plasmids shows that there is a wide range of copies in the host cells (**Figure S1D**). Roughly 50% of the host cells contain more than a four-fold difference in the numbers of plasmids (where $N_{P1}/(N_{P1}+N_{P2})$ is smaller than 0.2 or larger than 0.8). This result is consistent with the phenomenon of incompatibility between plasmids containing similar replication origins. In other words, because of competition for the RNA primer *RNAII* to initiate replication (9), there is a tendency for one plasmid to be preferred and dominate replication machinery. However, even with this incompatibility, only 10% of the cells exhibited a differentiable single plasmid from the majority ($N_{P1} = 1$ or $N_{P2} = 1$), which was not sufficient to conduct our experiments and required the addition of replication control.

Reference

1. Cox, R. S., 3rd, M. J. Dunlop, and M. B. Elowitz. 2010. A synthetic three-color scaffold for monitoring genetic regulation and noise. Journal of biological engineering 4:10.
2. Lau, I. F., S. R. Filipe, B. Søballe, O.-A. Ø kstad, F.-X. Barre, and D. J. Sherratt. 2004. Spatial and temporal organization of replicating Escherichia coli chromosomes. Molecular microbiology 49(3):731-743.
3. Panayotatos, N. 1984. DNA replication regulated by the priming promoter. Nucleic acids research 12(6):2641-2648.
4. Brenowitz, M., N. Mandal, A. Pickar, E. Jamison, and S. Adhya. 1991. DNA-binding properties of a lac repressor mutant incapable of forming tetramers. The Journal of biological chemistry 266(2):1281-1288.
5. Shi, J., and D. P. Biek. 1995. A versatile low-copy-number cloning vector derived from plasmid F. Gene 164(1):55-58.
6. Wang, Y., P. Penkul, and J. N. Milstein. 2016. Quantitative localization microscopy reveals a novel organization of a high-copy number plasmid. Biophysical journal 111(3):467-479.
7. Skulj, M., V. Okrslar, S. Jalen, S. Jevsevar, P. Slanc, B. Strukelj, and V. Menart. 2008. Improved determination of plasmid copy number using quantitative real-time PCR for monitoring fermentation processes. Microbial cell factories 7:6.
8. Velappan, N., D. Sblattero, L. Chasteen, P. Pavlik, and A. R. Bradbury. 2007. Plasmid incompatibility: more compatible than previously thought? Protein engineering, design & selection : PEDS 20(7):309-313.
9. Eguchi, Y., T. Itoh, and J. Tomizawa. 1991. Antisense RNA. Annual Review of Biochemistry 60(1):631-652.
10. Datsenko, K. A., and B. L. Wanner. 2000. One-step inactivation of chromosomal genes in Escherichia coli K-12 using PCR products. Proceedings of the National Academy of Sciences of the United States of America 97(12):6640-6645.

Table S1 Bacterial strains and plasmids

Strain or plasmid	Sequence	Source
Strain		
BW25113	*F-*, *Δ(araD-araB)567*, *ΔlacZ4787(::rrnB-3)*, *λ-*, *rph-1*, *Δ(rhaD-rhaB)568*, *hsdR514*	E. coli Genetic Stock Center (10)
BW25113FH	BW25113/ p15AA-phlFH.tq	This study
Plasmid		
pJMJ178	*P15A*, P_c::*araC*, P_{BAD}::*lacI-gfp*, *cat*	Gift from Dr. Kenn Gerdes
p15AA-phlFH.tq	*P15A*, P_c::*araC*, P_{BAD}::*phlF*, P_{J23119}::*hupA-mturquoise*, *bla*	This study
pSOT37	*ColE1*, P_{lac}::*minD minE-cypet*, *lacZ'::lacY'*, *bla*	Gift from Dr. Chia-Fu Chou
pTetR4-4m	*ColE1*, P_{tet}::*tetR-myfp*, *aphA*	This study
pTetORK34b	*ColE1*, P_{tet}::*tetR-myfp*, *tetO2*x54, *aphA*	This study
pLacI2-2	*ColE1*, P_{lac}::$lacI^{adi}$-*mcherry*, *cat*	This study
pLacOIC2c	*ColE1*, P_{lac}::$lacI^{adi}$-*mcherry*, *lacO2*x90, *cat*	This study
pTetR4-4p	*ColE1 Δ*P_{RNAII}:: P_{phlF}, P_{tet}::*tetR-myfp*, *aphA*	This study
pTetORK34p	*ColE1 Δ*P_{RNAII}:: P_{phlF}, P_{tet}::*tetR-myfp*, *tetO2*x54, *aphA*	This study
pZC320-tetO	*mini-F*, P_{tet}::*tetR-myfp*, *tetO2*x54, *bla*	This study
pZC320-lacO	*mini-F*, P_{lac}::$lacI^{adi}$-*mcherry*, *lacO2*x90, *bla*	This study

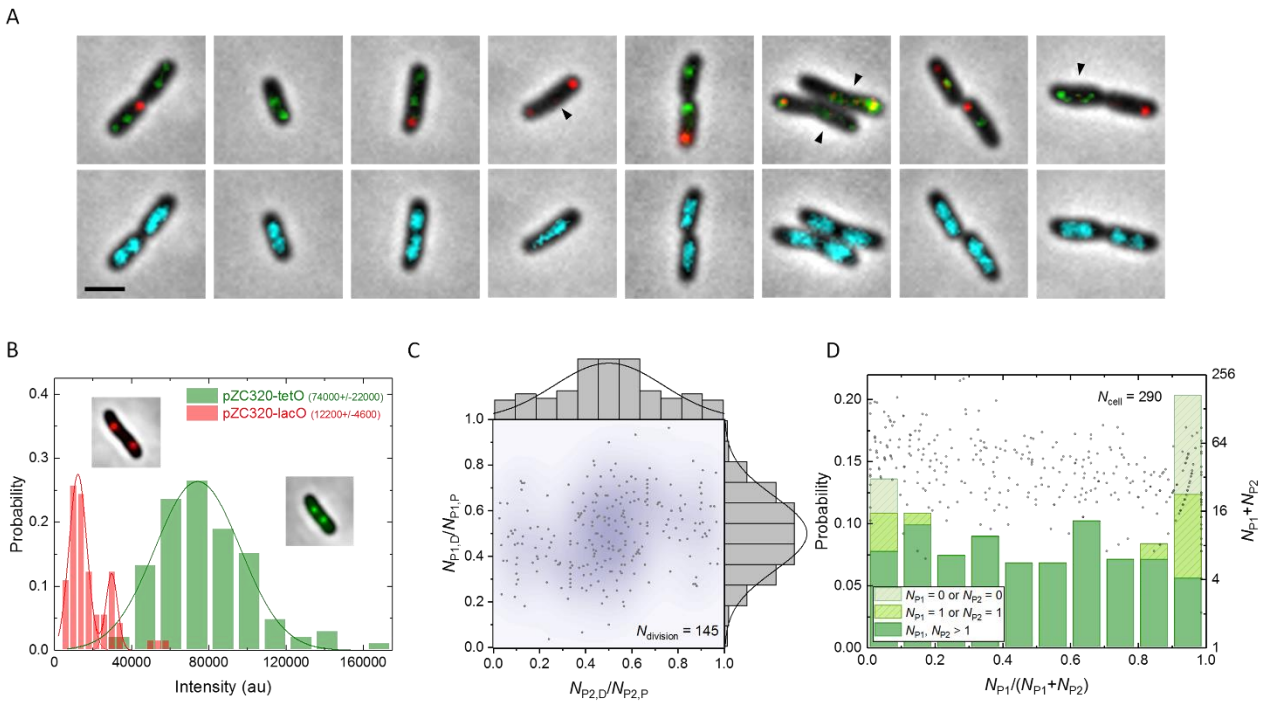

Figure S1. The applicability of the two-color self-regulated FROS on plasmids (pTetORK34b and pLacOIC2c) co-transformed in cells. (*A*) The merged sets of phase contrast images and fluorescence images show co-transformed plasmids pTetORK34b (P1; upper panel, green) and pLacOIC2c (P2; upper panel, red), as well as the nucleoids (lower panel, cyan). The arrows indicate possible single plasmids traveling around the nucleoids. The scale bar equals 2 μm. (*B*) The calibration of the fluorescence intensity by single self-regulated FROS plasmids. The measurement was made on cells transformed with single-copy plasmids, pZC320-tetO and pZC320-lacO, which encode the FROS genes, TetR-mYFP/*tetO*x54 (green; N = 116) and LacI^{adi}-mCherry/*lacO*x90 (red; N = 77), respectively. The overlap of plasmids is resolvable as a second peak in the fluorescence intensity of pZC320-lacO. (*C*) The correlation between the inherited ratio of pTetORK34b (P1) and pLacOIC2c (P2). Each spot indicates the quantity ratios, $N_{P1,D}/N_{P1,P}$ and $N_{P2,D}/N_{P2,P}$, from a single daughter cell and its parent cell. The density plot represents the probability density distribution. The individual probability densities of $N_{P1,D}/N_{P1,P}$ and $N_{P2,D}/N_{P2,P}$ are shown as the right and upper panels, respectively. The similar distributions and weak correlation (correlation coefficient ~ 0.22) suggest that P1 and P2 are physiologically identical with regard to segregation. (*D*) The total quantities (spots for single cells; right axis) and the corresponding probability histogram (bar chart; left axis) to the portion of pTetORK34b (P1) in all plasmids. In the probability histogram, the portions of cells without or with a single pTetORK34b (leftmost bars) or pLacOIC2c (P2; rightmost bars) are marked individually. Incidentally, the asymmetry between pTetORK34b and pLacOIC2c may be due to differences in antibiotic selection.

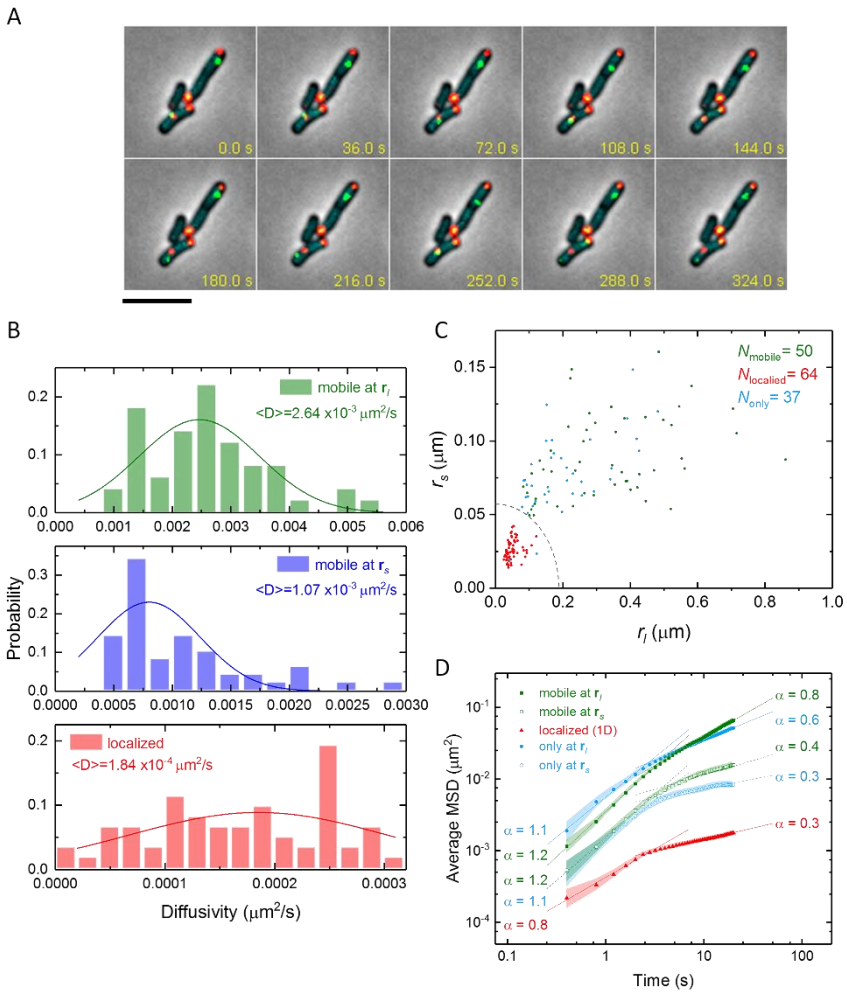

Figure S2. Plasmid motion resolved by single plasmid tracking. (*A*) An image sequence of nucleoids (dim cyan), plasmids pTetORK34p (green) and pLacOIC2c (red), and the cell outlines (phase contrast; gray) is shown. Each of the green spots is a single pTetORK34p plasmid, and the overlap of pTetORK34p and pLacOIC2c is shown in yellow. To better visualize single plasmids, the green fluorescent intensity has been multiplied 12-fold with respect to **Figure 1A** and **S1A**. The scale bar equals 5 μm. (*B*) The diffusion coefficients of the localized plasmids (red), as well as for mobile plasmids along the long (green) and short (blue) characteristic axes. The diffusion coefficients were calculated from the linear fits of the mean square displacements of single trajectories where $\tau \leq 2$. (*C*) A scatter plot shows the characteristic lengths of the 5-min trajectories of single localized (red) and mobile (green) PTetORK34p plasmids from **Figure 2B**, as well as those in cells containing only one pTetORK34p plasmid (cyan). (*D*) The average mean square displacements of the localized (red) and mobile (green) pTetORK34p plasmids, as well as the cells with only one pTetORK34p copy (cyan). The long (solid) and short (dashed) axes of the mobile and single plasmids were analyzed separately. The color bands represent the standard errors of the means. The distribution in (*C*) and the behaviors in (*D*) of the single plasmids are similar to those of the mobile plasmids and contrast with those of localized plasmids.

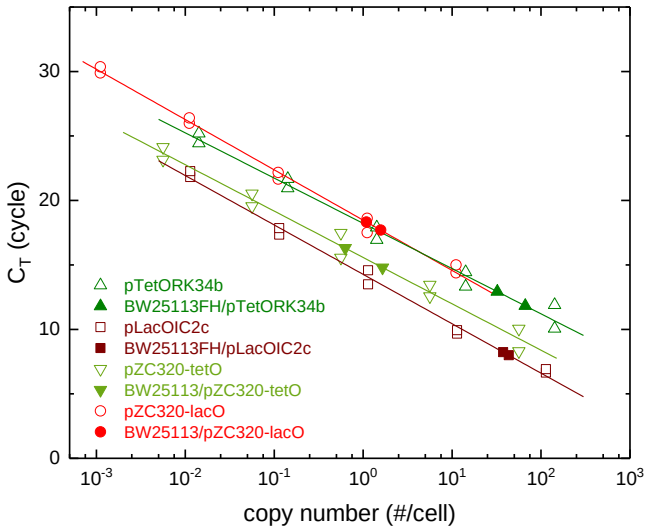

Figure S3. Average plasmid numbers of pTetORK34b (dim green), pLacOIC2c (dim red), pZC320-tetO (light green), and pZC320-lacO (light red) in cells measured by quantitative PCR. The standard curves were the linear-log fits of the measurements of the known plasmid concentrations (hollow spots), of which effective copy numbers were calculated from the cell concentrations of the respective cell samples. The standard curves were applied to estimate the copy numbers per bacterial cell in the cell samples (solid spots). The average numbers of pTetORK34b and pLacOIC2c were approximately 40, and those of pZC320-tetO and pZC320-lacO were about 1.

Description of supplemental videos

VideoS1. Two-color self-regulated FROS on co-transformed plasmids in live cells (BW25113FH/ pTetORK34b, pLacOIC2c). Respective colors: nucleoids (blue), plasmids pTetORK34b (green) and pLacOIC2c (red), and cell outlines (phase contrast; gray).

VideoS2. Five minutes of motion of single pTetORK34p plasmids in live cells (BW25113FH/pTetORK34p, pLacOIC2c) during the cell cycle. Respective colors: nucleoids (cyan), plasmids pTetORK34b (green) and pLacOIC2c (red), and cell outlines (phase contrast; gray).

VideoS3. Typical motion of a single pTetORK34p plasmid during the cell cycle (BW25113FH/ pTetORK34p, pLacOIC2c). Respective colors: nucleoids (cyan), plasmids pTetORK34p (green), and cell outlines (phase contrast; gray).